Acta Crystallographica Section C
Crystal Structure Communications
ISSN 0108-2701

1-(2-Cyclohex-2-enylpropionyl)-3-methylurea, 2-ethyl-5-methylhexanamide and 2-ethylpentanamide: three products of barbiturate decomposition

Gary S. Nichol*‡ and William Clegg

School of Chemistry, Newcastle University, Newcastle upon Tyne NE1 7RU, England
Correspondence e-mail: gsnichol@email.arizona.edu

Received 23 November 2010
Accepted 25 November 2010
Online 8 December 2010

The three title compounds were obtained by reactions which mimic, with more extreme conditions, the *in vivo* metabolism of barbiturates. 1-(2-Cyclohex-2-enylpropionyl)-3-methylurea, $C_{11}H_{18}N_2O_2$, (I), and 2-ethylpentanamide, $C_8H_{17}NO$, (III), both crystallize with two unique molecules in the asymmetric unit; in the case of (III), one unique molecule exhibits whole-molecule disorder. 2-Ethyl-5-methylhexanamide, $C_9H_{19}NO$, (II), crystallizes as a fully ordered molecule with $Z' = 1$. In the crystal structures, three different hydrogen-bonding motifs are observed: in (I) a combination of $R_2^2(4)$ and $R_2^2(8)$ motifs, and in (II) and (III) a combination of $R_4^2(8)$ and $R_2^2(8)$ motifs. In all three structures, one-dimensional ribbons are formed by N—H···O hydrogen-bonding interactions.

Comment

Substituted barbiturates have for decades been used as sedatives in the treatment of anxiety disorders (Volwiler & Tabern, 1930; Schwartz *et al.*, 2005). Their chemical and structural properties are much studied, polymorphism in particular (Zencirci *et al.*, 2009; Gryl *et al.*, 2008; Bernstein, 2002). Despite their widespread medical use and the extensive structural characterization of the drug molecules, charting the *in vivo* metabolic pathway and the subsequent identification of the resulting metabolites seem to have received much less attention, at least in terms of published material. A search of SciFinder Scholar in November 2010 for 'barbiturate metabolism' returned just 50 hits. In 1961 Freifelder and co-workers charted the synthetic route of the ring opening and subsequent hydrolysis of 5,5-disubstituted barbiturates (see reaction scheme); they had thus described a chemical model for the *in vivo* metabolism of barbiturates (Freifelder *et al.*, 1961).

Our interest in barbiturate crystal packing has revealed phase transitions (Nichol & Clegg, 2005*a*,*b*), metal complexes (Nichol & Clegg, 2005*c*), hydrogen-bonding interactions in organic co-crystals (Nichol & Clegg, 2006, 2009) and now the

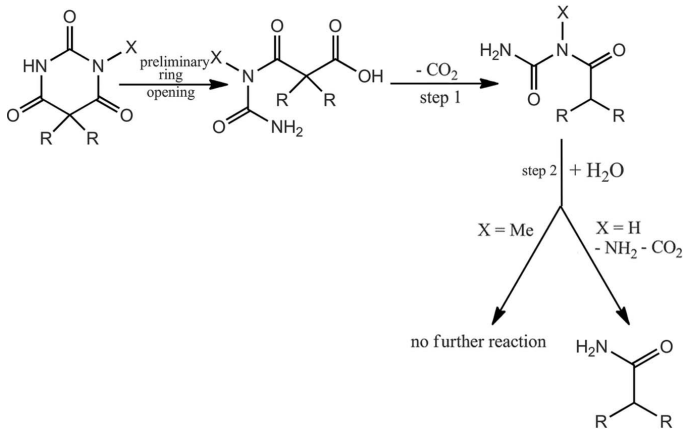

products of barbiturate hydrolysis. To investigate how the hydrogen-bonding motifs vary among barbiturate metabolites, we synthesized and characterized by X-ray crystallography the decomposition products of three 5,5-disubstituted barbituric acids (hexobarbitone, amylobarbitone and butobarbitone; see reaction scheme) according to the mechanism reported by Freifelder. In each case, the crystals obtained were of good size and sufficient quality that one would reasonably expect standard laboratory X-ray equipment to be satisfactory for data collection. This turned out to be incorrect and much

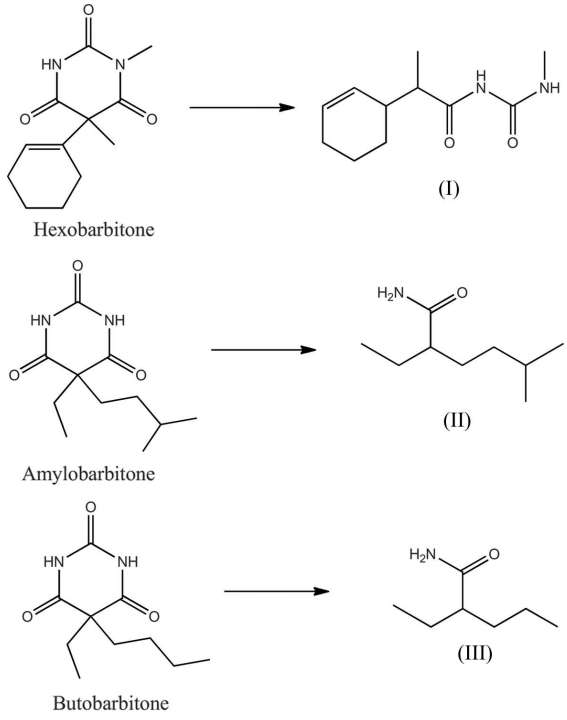

higher intensity radiation was necessary; data for one compound were collected using radiation from a rotating anode amplified by mirror optics (Coles & Hursthouse, 2004) at Southampton University *via* the EPSRC National X-ray Crystallography Service, and data for the other two

‡ Present address: Department of Chemistry and Biochemistry, The University of Arizona, 1306 E. University Boulevard, Tucson, AZ 85721, USA.

 doi:10.1107/S0108270110049322

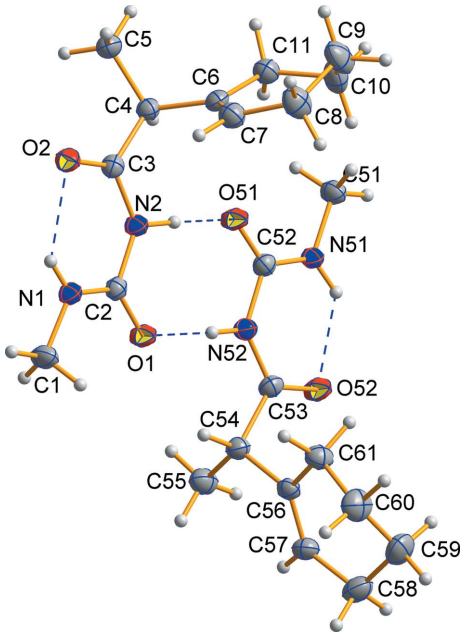

Figure 1
The asymmetric unit of (I), with displacement ellipsoids drawn at the 50% probability level. Dashed lines indicate hydrogen bonds.

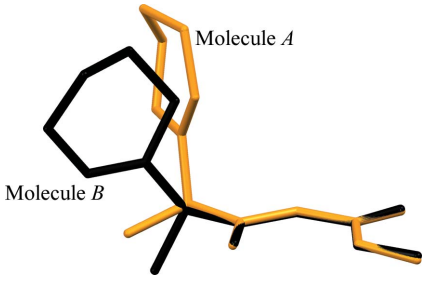

Figure 2
A least-squares overlay formed by fitting the urea groups of molecules *A* and *B* in (I), with an r.m.s. deviation of 0.04 Å. H atoms have been omitted.

compounds were collected at Station 9.8 of the Synchrotron Radiation Source (SRS) at Daresbury Laboratory.

The discussion below describes the hydrogen-bonding motifs in terms of graph-set notation (Bernstein *et al.*, 1995). The most pertinent pattern in this study is the $R_d^a(n)$ notation, where R = ring, a = number of acceptors, d = number of donors and n = total number of atoms in the ring. In addition, there are motifs of type S (intramolecular hydrogen bonding).

The synthesis of compound (I), 1-(2-cyclohex-2-enylpropionyl)-3-methylurea, is slightly different from that of the other two compounds, (II) and (III). The presence of an *N*-methyl group means that hydrolysis (step 2 of the reaction scheme) cannot proceed, so instead crystals of the product of the first decarboxylation are obtained. The molecular structure of (I) is presented in Fig. 1 and hydrogen-bonding details are given in Table 1. There are two crystallographically unique molecules in the asymmetric unit; the molecule composed of atoms O1 to C11 will henceforth be referred to as molecule *A* and the molecule composed of atoms O51 to C61 as molecule *B*. Discussion is focused on molecule *A* with results for molecule

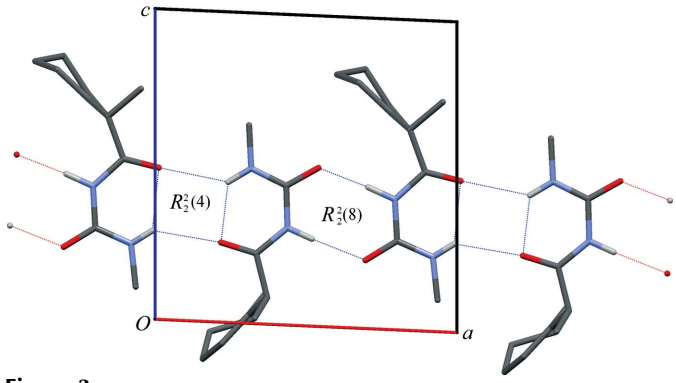

Figure 3
The intermolecular hydrogen bonding in (I). Dotted lines indicate hydrogen bonding and dotted lines at the edges of the figure indicate hydrogen-bonding continuation.

B given in parentheses. Within the molecule, the urea group is essentially planar, with an r.m.s. deviation of 0.022 Å (0.016 Å); the two molecules differ in the orientations of the cyclohex-2-enyl groups, as a result of free rotation about the C3—C4 (C53—C54) bond. Fig. 2 shows a least-squares overlay formed by fitting the urea groups of molecules *A* and *B*, with an r.m.s. deviation of 0.04 Å. The differences in the cyclohex-2-enyl orientations are clear; both cyclohex-2-enyl rings adopt a half-chair conformation.

In the crystal structure, N—H···O hydrogen bonding links adjacent unique molecules to form a one-dimensional ribbon which propagates parallel with the *a* axis (Fig. 3). In addition to an $S(6)$ interaction found in both molecules, two intermolecular hydrogen-bonding motifs are present, *viz.* an $R_2^2(8)$ motif, common between amide groups, and a second $R_2^2(4)$ motif. This combination of ring motifs, to yield a one-dimensional ribbon, has also been observed in other urea derivatives (Hashizume *et al.*, 2003; Chen *et al.*, 2005). Bond angles around the carbonyl C atom deviate significantly from 120°; this is also consistent with other urea derivatives with the same hydrogen-bonding pattern.

Compound (II), 2-ethyl-5-methylhexanoic acid amide, was synthesized from amylobarbitone; in amylobarbitone there is no *N*-methyl group and so hydrolysis can proceed to give the final acid amide product. As a result there are only one

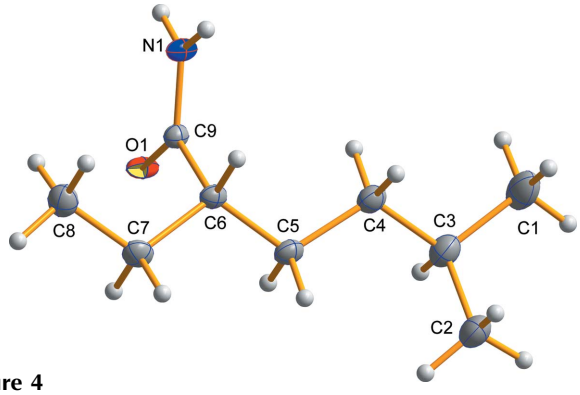

Figure 4
The asymmetric unit of (II), with displacement ellipsoids drawn at the 30% probability level.

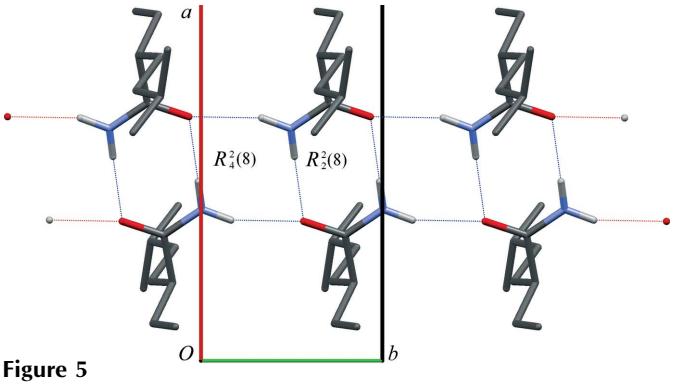

Figure 5
Hydrogen-bonding patterns in (II). Dotted lines indicate hydrogen bonding and dotted lines at the edges of the figure indicate hydrogen-bonding continuation.

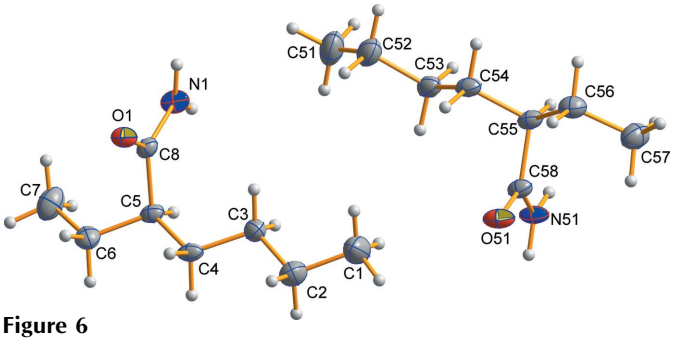

Figure 6
The asymmetric unit of (III), with displacement ellipsoids drawn at the 30% probability level; the minor disorder component has been omitted.

hydrogen-bond acceptor and two donor sites, which means that the range of potential motifs is much more limited than those possible in compound (I). The molecular structure of (II) is shown in Fig. 4, and molecular dimensions are unexceptional. Hydrogen-bonding details are given in Table 2. In the crystal structure, each carbonyl group acts as a bifurcated hydrogen-bond acceptor and both H atoms of each amine group act as hydrogen-bond donors; thus, all potential hydrogen-bonding donors and acceptors are satisfied. Two different hydrogen-bonding motifs are present (Fig. 5): an $R_2^2(8)$ interaction is found as in (I), and an $R_4^2(8)$ motif links the dimers into an infinite tape which runs parallel to the *b* axis.

Compound (III), 2-ethylpentanamide, was synthesized from butobarbitone; as with amylobarbitone, butobarbitone contains no *N*-methyl group and consequently the product of hydrolysis, (III), is analogous to (II). The molecular structure of (III) is presented in Fig. 6 and hydrogen-bonding geometry is given in Table 3. The unit-cell parameters for (III) are also similar to those of (II). However, where (II) crystallizes in the space group *C*2/*c*, (III) crystallizes in the space group $P2_1/c$ with two crystallographically independent molecules (molecule *A* formed by atoms O1 to C8 and molecule *B* formed by atoms O51 to C58) in the asymmetric unit and overall $Z = 8$. There are no exact or approximate systematic absences in the data for (III) which would suggest a centred unit cell. Molecule *A* exhibits whole-molecule disorder; this was modelled over two sites and refined with occupancies of 0.559 (8): 0.441 (8). Molecule *B* is fully ordered. Hydrogen-bonding patterns are the same as for (II) (Fig. 5) and the overall crystal packing is broadly similar.

Experimental

The 5,5-disubstituted barbituric acids were obtained as commercial samples from Professor Roger Griffin, Newcastle University. Caesium hydroxide monohydrate was purchased from Lancaster Chemicals. All reagents were used without further purification. For the preparation of (I), hexobarbitone (0.223 g, 0.94 mmol) and $CsOH·H_2O$ (0.169 g, 1 mmol) were dissolved in boiling distilled water (40 ml). The solution was boiled until *ca* 15 ml remained when the hot solution was transferred to a separate sample vial and set aside to cool undisturbed at room temperature. Large colourless lath-shaped crystals of (I) appeared after approximately 2 weeks (yield: 35 mg, 17.7%). For the preparation of (II), amylobarbitone (0.228 g, 1 mmol) was placed in a Teflon-lined steel autoclave along with distilled water (10 ml). The sealed autoclave was placed in an oven and kept at 453 K for 48 h after which time the oven temperature was cooled slowly to 298 K over a period of 18 h. Large colourless lath-shaped crystals of (II) were removed from the autoclave and stored in distilled water (yield: 55 mg, 35.03%). For the preparation of (III), butobarbitone (0.219 g, 1 mmol) was placed in a Teflon-lined steel autoclave along with distilled water (10 ml). The sealed autoclave was placed in an oven and kept at 453 K for 48 h after which time the oven temperature was cooled slowly to 298 K over a period of 18 h. Large colourless lath-shaped crystals of (III) were removed from the autoclave and stored in distilled water (yield: 45 mg, 32.59%).

Compound (I)

Crystal data

$C_{11}H_{18}N_2O_2$
$M_r = 210.27$
Monoclinic, $P2_1/c$
$a = 10.108$ (2) Å
$b = 21.824$ (4) Å
$c = 10.393$ (2) Å
$\beta = 92.52$ (3)°
$V = 2290.4$ (8) Å^3
$Z = 8$
Mo $K\alpha$ radiation
$\mu = 0.09$ mm^{-1}
$T = 120$ K
0.36 × 0.08 × 0.03 mm

Data collection

Nonius KappaCCD diffractometer
Absorption correction: multi-scan (*SORTAV*; Blessing, 1995)
$T_{min} = 0.970$, $T_{max} = 0.998$
37076 measured reflections
4030 independent reflections
3184 reflections with $I > 2\sigma(I)$
$R_{int} = 0.110$

Refinement

$R[F^2 > 2\sigma(F^2)] = 0.058$
$wR(F^2) = 0.140$
$S = 1.09$
4030 reflections
292 parameters
H atoms treated by a mixture of independent and constrained refinement
$\Delta\rho_{max} = 0.26$ e Å^{-3}
$\Delta\rho_{min} = -0.23$ e Å^{-3}

Compound (II)

Crystal data

$C_9H_{19}NO$
$M_r = 157.25$
Monoclinic, $C2/c$
$a = 22.839$ (6) Å
$b = 5.0394$ (13) Å
$c = 18.802$ (5) Å
$\beta = 111.224$ (4)°
$V = 2017.2$ (9) Å^3
$Z = 8$
Synchrotron radiation
$\lambda = 0.6933$ Å
$\mu = 0.07$ mm^{-1}
$T = 120$ K
0.20 × 0.10 × 0.05 mm

Table 1
Hydrogen-bond geometry (Å, °) for (I).

D—H···A	D—H	H···A	D···A	D—H···A
N1—H1N···O2	0.84 (3)	2.14 (3)	2.732 (3)	127 (3)
N2—H2N···O51	0.98 (3)	1.81 (3)	2.781 (3)	171 (2)
N51—H51N···O52	0.90 (3)	2.04 (3)	2.692 (3)	128 (2)
N52—H52N···O1	0.89 (3)	1.95 (3)	2.837 (3)	175 (2)
N1—H1N···O52^{i}	0.84 (3)	2.35 (3)	3.032 (3)	139 (3)
N51—H51N···O2^{ii}	0.90 (3)	2.38 (3)	3.109 (3)	138 (2)

Symmetry codes: (i) $x+1, y, z$; (ii) $x-1, y, z$.

Table 2
Hydrogen-bond geometry (Å, °) for (II).

D—H···A	D—H	H···A	D···A	D—H···A
N1—H1N···O1^{i}	0.88	2.07	2.9488 (18)	179
N1—H2N···O1^{ii}	0.88	2.02	2.8492 (18)	156

Symmetry codes: (i) $-x+\frac{1}{2}, -y+\frac{3}{2}, -z$; (ii) $x, y+1, z$.

Data collection

Bruker APEXII diffractometer
Absorption correction: multi-scan (*SADABS*; Sheldrick, 1996)
T_{min} = 0.987, T_{max} = 0.997
5147 measured reflections
1867 independent reflections
1456 reflections with $I > 2\sigma(I)$
R_{int} = 0.042

Refinement

$R[F^2 > 2\sigma(F^2)]$ = 0.054
$wR(F^2)$ = 0.159
S = 1.06
1867 reflections
103 parameters
H-atom parameters constrained
$\Delta\rho_{max}$ = 0.35 e Å^{-3}
$\Delta\rho_{min}$ = −0.18 e Å^{-3}

Compound (III)

Crystal data

$C_8H_{17}NO$
M_r = 143.23
Monoclinic, $P2_1/c$
a = 21.597 (5) Å
b = 5.0469 (12) Å
c = 18.424 (5) Å
β = 111.529 (3)°
V = 1868.0 (8) Å^3
Z = 8
Synchrotron radiation
λ = 0.6933 Å
μ = 0.04 mm^{-1}
T = 120 K
0.20 × 0.10 × 0.05 mm

Data collection

Bruker APEXII diffractometer
Absorption correction: multi-scan (*SADABS*; Sheldrick, 1996)
T_{min} = 0.992, T_{max} = 0.998
12823 measured reflections
3250 independent reflections
2184 reflections with $I > 2\sigma(I)$
R_{int} = 0.052

Refinement

$R[F^2 > 2\sigma(F^2)]$ = 0.049
$wR(F^2)$ = 0.141
S = 1.02
3250 reflections
274 parameters
19 restraints
H-atom parameters constrained
$\Delta\rho_{max}$ = 0.17 e Å^{-3}
$\Delta\rho_{min}$ = −0.13 e Å^{-3}

All H atoms were first located in a difference Fourier map. In (I), N-bound H atoms were freely refined. In (II) and (III), N-bound H atoms were refined as riding atoms, with U_{iso}(H) = 1.5U_{eq}(N) and a fixed N—H distance of 0.88 Å. In all structures, C-bound H atoms were refined as riding, with U_{iso}(H) = 1.2U_{eq}(C) [or 1.5U_{eq}(C) for methyl H atoms] and fixed C—H distances (0.95–1.00 Å). Molecule *A* in the asymmetric unit of compound (III) exhibits whole-molecule disorder, which was refined over two positions with an occupancy ratio of 0.559 (8):0.441 (8). Bond distance similarity restraints with a tolerance standard deviation of 0.02 Å were used to control the refinement of the disordered molecule. Real and imaginary components of the anomalous scattering factors for (II) and (III) were calculated using *WinGX* (Farrugia, 1999).

Table 3
Hydrogen-bond geometry (Å, °) for (III).

D—H···A	D—H	H···A	D···A	D—H···A
N1—H1N···O51^{i}	0.88	1.99	2.858 (15)	170
N1—H2N···O1^{ii}	0.88	2.06	2.901 (12)	160
N51—H51*B*···O51^{ii}	0.88	2.03	2.8539 (19)	156
N51—H51*A*···O1^{iii}	0.88	2.10	2.980 (10)	179

Symmetry codes: (i) $x, -y+\frac{3}{2}, z+\frac{1}{2}$; (ii) $x, y+1, z$; (iii) $x, -y+\frac{3}{2}, z-\frac{1}{2}$.

Data collection: *COLLECT* (Nonius, 1998) for (I); *APEX2* (Bruker, 2007) for (II) and (III). Cell refinement: *DENZO* (Otwinowski & Minor, 1997) for (I); *APEX2* for (II) and (III). Data reduction: *DENZO* and *SCALEPACK* (Otwinowski & Minor, 1997) for (I); *APEX2* for (II) and (III). For all compounds, program(s) used to solve structure: *SHELXTL* (Sheldrick, 2008); program(s) used to refine structure: *SHELXTL*; molecular graphics: *DIAMOND* (Brandenburg & Putz, 1999) and *Mercury* (Macrae *et al.*, 2008); software used to prepare material for publication: *SHELXTL*, *publCIF* (Westrip, 2010) and local programs.

The authors thank the staff of the EPSRC National X-ray Crystallography Service at Southampton University for data collection and processing for (I). Drs Ross Harrington, Luca Russo and Zhanhui Yuan are thanked for data collection and processing for (II) and (III) at Station 9.8, SRS, Daresbury Laboratory, as part of the EPSRC National X-ray Crystallography Service synchrotron component operated from Newcastle University. We thank Professor Roger Griffin, Newcastle University, for supplying the barbiturates for our research, the EPSRC for funding of a studentship and the National Crystallography Service, and CCLRC (now STFC) for access to synchrotron facilities.

Supplementary data for this paper are available from the IUCr electronic archives (Reference: SK3397). Services for accessing these data are described at the back of the journal.

References

Bernstein, J. (2002). *Polymorphism in Molecular Crystals*. New York: Oxford University Press.
Bernstein, J., Davis, R. E., Shimoni, L. & Chang, N.-L. (1995). *Angew. Chem. Int. Ed. Engl.* **34**, 1555–1573.
Blessing, R. H. (1995). *Acta Cryst.* A**51**, 33–38.
Brandenburg, K. & Putz, H. (1999). *DIAMOND*. Crystal Impact GbR, Bonn, Germany.
Bruker (2007). *APEX2*. Bruker AXS Inc., Madison, Wisconsin, USA.
Chen, L., Wang, Q., Huang, R., Mao, C., Shang, J. & Song, H. (2005). *Appl. Organomet. Chem.* **19**, 45–48.
Coles, S. J. & Hursthouse, M. B. (2004). *J. Appl. Cryst.* **37**, 988–992.
Farrugia, L. J. (1999). *J. Appl. Cryst.* **32**, 837–838.
Freifelder, M., Geiszler, A. O. & Stone, G. R. (1961). *J. Org. Chem.* **26**, 203–206.

Gryl, M., Krawczuk, A. & Stadnicka, K. (2008). *Acta Cryst.* B**64**, 623–632.
Hashizume, D., Miki, N., Yamazaki, T., Aoyagi, Y., Arisato, T., Uchiyama, H., Endo, T., Yasui, M. & Iwasaki, F. (2003). *Acta Cryst.* B**59**, 404–415.
Macrae, C. F., Bruno, I. J., Chisholm, J. A., Edgington, P. R., McCabe, P., Pidcock, E., Rodriguez-Monge, L., Taylor, R., van de Streek, J. & Wood, P. A. (2008). *J. Appl. Cryst.* **41**, 466–470.
Nichol, G. S. & Clegg, W. (2005*a*). *Acta Cryst.* C**61**, o297–o299.
Nichol, G. S. & Clegg, W. (2005*b*). *Acta Cryst.* B**61**, 464–472.
Nichol, G. S. & Clegg, W. (2005*c*). *Acta Cryst.* C**61**, m459–m462.
Nichol, G. S. & Clegg, W. (2006). *Cryst. Growth Des.* **6**, 451–460.
Nichol, G. S. & Clegg, W. (2009). *Cryst. Growth Des.* **9**, 1844–1850.
Nonius (1998). *COLLECT*. Nonius BV, Delft, The Netherlands.
Otwinowski, Z. & Minor, W. (1997). *Methods in Enzymology*, Vol. 276, *Macromolecular Crystallography*, Part A, edited by C. W. Carter Jr & R. M. Sweet, pp. 307–326. New York: Academic Press.
Schwartz, T. L., Nihaamo, N., Simionescu, M. & Hopkins, G. (2005). *Curr. Pharm. Des.* **11**, 255–263.
Sheldrick, G. M. (1996). *SADABS*. University of Göttingen, Germany.
Sheldrick, G. M. (2008). *Acta Cryst.* A**64**, 112–122.
Volwiler, E. H. & Tabern, D. L. (1930). *J. Am. Chem. Soc.* **52**, 1679.
Westrip, S. P. (2010). *J. Appl. Cryst.* **43**, 920–925.
Zencirci, N., Gelbrich, T., Kahlenberg, V. & Griesser, U. J. (2009). *Cryst. Growth Des.* **9**, 3444–3456.